The Journal of Headache and Pain

RESEARCH

Open Access

Cerebral perfusion variance in new daily persistent headache and chronic migraine: an arterial spin-labeled MR imaging study

Xiaoyan Bai[1,2†] ⓘ, Wei Wang[3†] ⓘ, Xueyan Zhang[4†] ⓘ, Zhangxuan Hu[5], Yingkui Zhang[1], Zhiye Li[1,2], Xue Zhang[1,2], Ziyu Yuan[3], Hefei Tang[3], Yaqing Zhang[3], Xueying Yu[3], Peng Zhang[3], Yonggang Wang[3*] and Binbin Sui[1*]

Abstract

Background and purpose: New daily persistent headache (NDPH) and chronic migraine (CM) are two different types of headaches that might involve vascular dysregulation. There is still a lack of clarity about altered brain perfusion in NDPH and CM. This study aimed to investigate the cerebral perfusion variances of NDPH and CM using multi-delay pseudo-continuous arterial spin-labeled magnetic resonance imaging (pCASL-MRI).

Methods: Fifteen patients with NDPH, 18 patients with CM, and 15 age- and sex-matched healthy controls (HCs) were included. All participants underwent 3D multi-delay pCASL-MRI to obtain cerebral perfusion data, including arrival-time-corrected cerebral blood flow (CBF) and arterial cerebral blood volume (aCBV). The automated anatomical labeling atlas 3 (AAL3) was used to parcellate 170 brain regions. The CBF and aCBV values in each brain region were compared among the three groups. Correlation analyses between cerebral perfusion parameters and clinical variables were performed.

Results: Compared with HC participants, patients with NDPH were found to have decreased CBF and aCBV values in multiple regions in the right hemisphere, including the right posterior orbital gyrus (OFCpost.R), right middle occipital gyrus (MOG.R), and ventral anterior nucleus of right thalamus (tVA.R), while patients with CM showed increased CBF and aCBV values presenting in the ventral lateral nucleus of left thalamus (tVL.L) and right thalamus (tVL.R) compared with HCs (all $p < 0.05$). In patients with NDPH, after age and sex adjustment, the increased aCBV values of IFGorb. R were positively correlated with GAD-7 scores; and the increased CBF and aCBV values of tVA.R were positively correlated with disease duration.

Conclusion: The multi-delay pCASL technique can detect cerebral perfusion variation in patients with NDPH and CM. The cerebral perfusion changes may suggest different variations between NDPH and CM, which might provide hemodynamic evidence of these two types of primary headaches.

---

†Xiaoyan Bai, Wei Wang and Xueyan Zhang contributed equally to this work.

*Correspondence: w100yg@163.com; Reneesui@163.com

[1] Tiantan Neuroimaging Center for Excellence, China National Clinical Research Center for Neurological Diseases, Beijing Tiantan Hospital, Capital Medical University, No.119 South Fourth Ring West Road, Fengtai District, Beijing 100070, China
[3] Headache Center, Department of Neurology, Beijing Tiantan Hospital, Capital Medical University, No.119 South Fourth Ring West Road, Fengtai District, Beijing 100070, China
Full list of author information is available at the end of the article

Bai *et al. The Journal of Headache and Pain*   (2022) 23:156

Page 2 of 13

Introduction

New daily persistent headache (NDPH) is a new-onset primary headache with a clearly remembered onset, characterized by persistent headache that is continuous and unremitting within 24 hours and then persists on a daily basis for more than 3 months [1]. In community-based settings, two studies from Spain and Norway reported that the 1-year prevalence of NDPH was 0.1% [2] and 0.03% [3], respectively. Although rare, NDPH is one of the most treatment-refractory primary headache disorders, and may significantly affect the individual's quality of life and can lead to psychiatric comorbidity [4]. Similarly, as a disabling disease, Chronic migraine (CM) is defined as headaches on at least 15 days per month for more than 3 months, with at least eight headache days per month fulfilling the criteria for migraine headaches [1]. It affects 1.4–2.2% of the general population and is a significant impact on the socioeconomic functioning and life quality of patients [5]. These two types of headache diseases have drawn more and more attention in late years, but the underlying pathophysiology mechanisms of NDPH and CM are still unclear. The elucidation of the underlying pathophysiological mechanisms will help early accurate diagnosis and treatment strategies.

The pathophysiology mechanisms of migraine chronification, including the atypical pain processing, cortical hyperexcitability, inflammation and central sensitization, have been studied [6, 7]. And the pathogenesis of NDPH was thought to be related to the stimulation of inflammatory factors secondary to CNS inflammation [2]. However, in recent years, more and more ground has been received by the "neurovascular hypothesis", assuming an interplay of both vascular and neuronal factors to be involved in the development of migraine [8, 9]. Some studies have shown that headache is a neurovascular disease, and abnormal hemodynamics caused by neurovascular dysfunction may be one of the pathological mechanisms of headache [9–12]. A recent CM study using 3D pseudo-continuous arterial spin labeling (3D pCASL) imaging detected hypoperfusion of the left nucleus accumbens [10]. However, cerebral hemodynamic investigation was still rarely reported in CM, and there was no report of the cerebral hemodynamic features in NDPH. As we all know, NDPH and CM are both primary chronic headache disorders, but some evidence suggested that NDPH has distinct clinical features, risk factors, therapeutic options, and prognosis compared with CM [2, 6]. At present, the comparative study of the hemodynamic status in these two types of primary chronic headaches has not been reported. Therefore, we would like to investigate whether these two types of chronic headaches would present with hemodynamic variances. In particular, we would like to focus on the hemodynamic status of NDPH and compare whether there are different hemodynamic characteristics between NDPH and CM in this preliminary study.
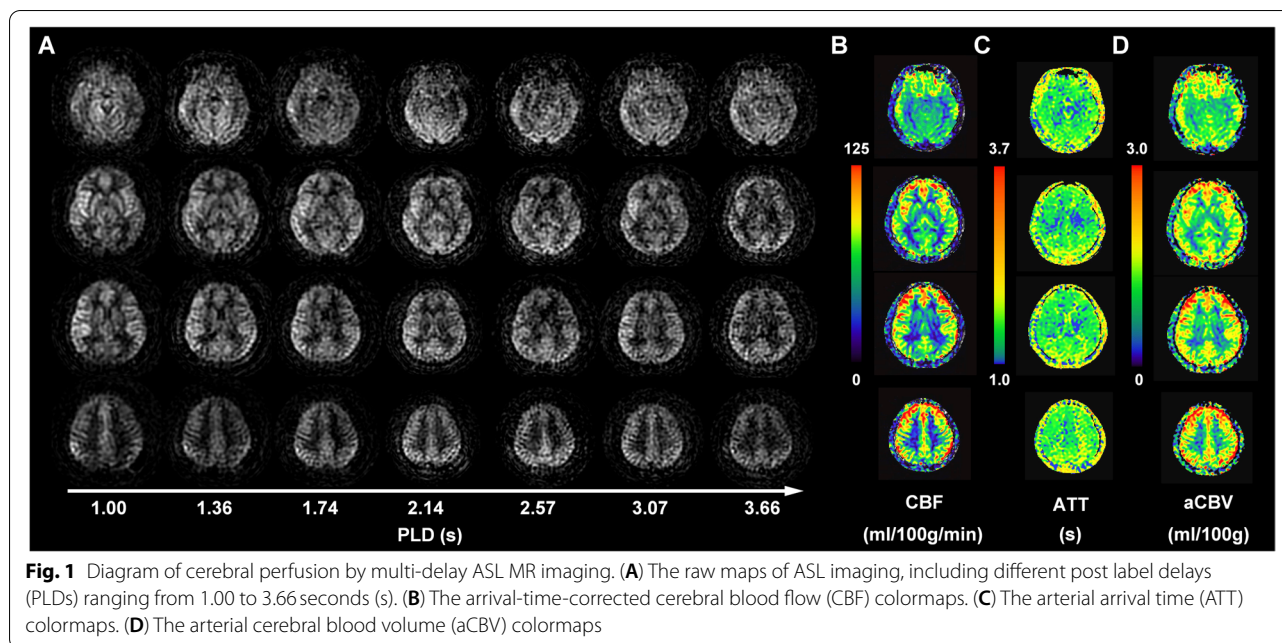
Arterial spin labeling (ASL) is a magnetic resonance (MR) imaging technique that enables assessing brain perfusion without applying an exogenous contrast agent. The reliability and reproducibility of ASL in cerebral perfusion measurement have been validated, with ASL results showing consistency with positron emission tomography (PET) and dynamic susceptibility contrast (DSC) [13–15]. Three-dimensional pseudo-continuous ASL (pCASL) has been adopted as the evaluation method of cerebral hemodynamics in clinical practice due to its ease of implementation and high signal-to-noise ratio (SNR) [16]. It has been widely applied in dementia, stroke, vascular malformations, and tumors [16–20]. Several studies have reported on the cerebral perfusion changes in episodic migraine and found abnormal regional hyperperfusion in gray matter [12, 21, 22]. Multi-delay pCASL, in which images with several post-label delay (PLD) times are taken for improvement of the accuracy of cerebral blood flow (CBF) quantification, has been applied to ischemic stroke, moyamoya disease, and idiopathic generalized epilepsy [23–25]. However, so far, less is known about the regional cerebral perfusion in primary chronic headache based on multi-delay 3D pCASL MR imaging (pCASL-MRI). We hypothesized that abnormal regional cerebral perfusion presents in NDPH and CM compared with HC, and cerebral perfusion characteristics differ between NDPH and CM.

In this study, we aimed to investigate the cerebral perfusion variance of NDPH and CM using multi-delay pCASL-MRI, and to evaluate the relationship between the cerebral perfusion parameters and clinical variables.

Methods

Participants

From October 2020 to April 2022, 16 healthy control participants (HC) and 35 patients who were diagnosed NDPH ($n=15$) and CM ($n=20$) were enrolled in the Headache Center, Department of Neurology, Beijing Tiantan Hospital, Capital Medical University. This work was approved by the Institutional Review Board

Bai *et al. The Journal of Headache and Pain* (2022) 23:156

Page 3 of 13

Fig. 1 Diagram of cerebral perfusion by multi-delay ASL MR imaging. (**A**) The raw maps of ASL imaging, including different post label delays (PLDs) ranging from 1.00 to 3.66 seconds (s). (**B**) The arrival-time-corrected cerebral blood flow (CBF) colormaps. (**C**) The arterial arrival time (ATT) colormaps. (**D**) The arterial cerebral blood volume (aCBV) colormaps

(KY2022–044) of Beijing Tiantan Hospital, Capital Medical University. All participants provided written informed consent prior to study enrolment. The study was registered with https://www.clinicaltrials.gov (unique identifier: NCT05334927). All of patients with CM were migraine without aura. The inclusion criteria for NDPH and CM were (1) the patients satisfy the definition of NDPH and CM according to the 3rd edition of the International Classification of Headache Disorders (ICHD-3) [1], (2) all participants ranged in age from 20 to 70 years. The exclusion criteria of NDPH and CM were as follows: (1) with other types of primary headache, (2) MRI claustrophobia or contraindications, (3) poor image quality, (4) history of alcohol or substance abuse, (5) brain damage or other neurological diseases (such as epilepsy, stroke, and physical disease) that can affect research results. The inclusion criteria for HCs were: (1) feasibility of MRI scan (no claustrophobic syndrome and no metal in the body); (2) no neurological or other major systemic diseases; (3) match age and sex to patients of NDPH and CM. The exclusion criteria of HCs were as follows: (1) pregnancy or breastfeeding; (2) MRI contraindications; (3) poor MRI data quality.

Demographic data were recorded for all participants. Clinical scales including the Headache Impact Test-6 (HIT-6), Patient Health Questionnaire-9 (PHQ-9), Generalized Anxiety Disorder-7 (GAD-7), and Pittsburgh Sleep Quality Index (PSQI) were assessed by an experienced neurologist and recorded in our headache questionnaire before the MRI data acquisition. HIT-6 [26] is designed to measure the impact and effect of headache on the ability to function normally in daily life, PHQ-9 [27] is designed to measure symptoms of depression in primary care settings, GAD-7 [28] is used to assess anxiety, and PSQI [29] is used to measure sleep quality and patterns.

MR imaging acquisition

MR imaging was performed on a 3 T MR scanner (Signa Premier, GE Healthcare, Waukesha, WI) using a 48-channel head coil. All participants were instructed to lie in a supine position, and formed padding was used to limit head movement. Volumetric perfusion imaging was obtained using a multi-delay pCASL sequence with spiral readout. The parameters were as follows: $TR = 7138$ ms; $TE = 11$ ms; slice thickness $= 4.5$ mm; $NEX = 1$; readout: 5 arms $\times 640$ samples; $FOV = 208$ mm $\times 208$ mm, and reconstruction matrix $= 128 \times 128$. The total examination time for the ASL protocol was 4 minutes 44 seconds. This protocol encodes seven different post-labeling delay (PLD) times into a single acquisition. Images with PLD times of 1.00, 1.36, 1.74, 2.14, 2.57, 3.07, and 3.66 seconds and effective label durations (LD) of 0.36, 0.38, 0.40, 0.44, 0.49, 0.59, and 0.84 seconds were acquired (Fig. 1).

Imaging analysis

The arterial transit time (ATT) maps can be estimated with signal weighted delay described by Dai et al. [30] For each pair of PLD and LD, the arrival-time-corrected CBF maps can be quantified as follows:

Bai *et al. The Journal of Headache and Pain* (2022) 23:156

Page 4 of 13

$$CBF = \frac{6000e^{\delta/T_{1a}}}{2\epsilon T_{1a}\left(e^{-\frac{\max(\omega-\delta,0)}{T_{1a}}} - e^{-\frac{\max(\tau+\omega-\delta,0)}{T_{1a}}}\right)}\frac{M}{M0},$$

in which δ is the arterial transit time, τ is the LD, ω is the PLD, T_{1a} is the longitudinal relaxation time of arterial blood (1.6 s), ϵ is the combined efficiency of labeling and background suppression (0.63), M is the signal intensity of the perfusion weighted image, and M0 is the signal intensity of the reference image. The final CBF was the mean of the estimated CBF at each pair of PLD and LD. Arterial cerebral blood volume (aCBV) maps were generated by the product of ATT and CBF, which indicates the arterial blood volume from the labeling plane to the imaging voxel [31]:

$$aCBV = CBF \bullet ATT$$

The arrival-time-corrected CBF and ATT maps were registered to the standard Montreal Neurologic Institute (MNI) stereotaxic space using Statistical Parametric Mapping 12 (SPM 12) (http://www.fil.ion.ucl.ac.uk/spm/) with the aid of M0 images acquired in ASL sequence. The automated anatomical labelling atlas 3 (AAL3) [32] was used to parcellate the brain into 170 regions. The mean CBF, ATT and aCBV values of gray matter in each region were calculated. The visualization of arrival-time-corrected CBF, ATT and aCBV colormaps is presented in Fig. 1.

Statistical analysis

The sample size was based on the available data and previous literature. A sample size of 30 cases (15 HC group and 15 CM group) would provide 80% power to reject the null hypothesis equal means when the mean difference is 5.49 (55.83–49.34) with standard deviations of 6.55 for HC group and 6.09 for CM group at a two-sided alpha of 0.05 [10]. Given an anticipated dropout rate of 20%, the total sample size required is 36 cases (18 HC group and 18 CM group). Fifteen NDPH cases were included in this study according to the previous similar studies [10, 21, 22, 33, 34]. To match the age and sex of patients with NDPH, 15 HC and 18 patients with CM were included in this study. All quantitative data were expressed as mean ± standard deviation (SD) for the normal distribution data or median with a range for the non-normal distribution data. The Kolmogorov–Smirnov test was used to test the normality of clinical data and cerebral perfusion parameters. Categorical variables were analyzed using the Chi-square test or Fisher's exact test. For the normally distributed data, comparisons of CBF and aCBV values among the three groups (HC, NDPH, and CM) were performed by one-way analysis of variance (ANOVA), and post hoc analysis with the Bonferroni correction method [35] was used for multiple comparisons. For the non-normally distributed data, comparisons of CBF and aCBV values in brain regions among the three groups were performed by the Kruskal-Wallis H test, and all pairwise comparisons were performed using Kruskal-Wallis 1-way ANOVA (k samples). Comparisons of clinical characteristics between the CM and NDPH groups were performed by the Independent Samples T-test for the normally distributed data and the Mann-Whitney U test for the non-normally distributed data. The correlations between clinical characteristics and brain regions with significant differences were determined using Pearson's or Spearman's correlation analysis with age and sex as covariates, depending on whether the data were normally or non-normally distributed. Positive and negative values of correlation coefficient r represent positive and negative correlations. A two-sided $P < 0.05$ was considered statistically significant. All statistical analyses were performed using SPSS 26.0 software (SPSS Inc., Chicago, IL, USA).

Results

Patient demographics and clinical characteristics

Fifty-one participants (16 HC, 15 NDPH, and 20 CM participants) were enrolled in this study. The patient enrollment flowchart is shown in Supplementary Fig. 1. Two patients with CM were excluded due to poor images ($n = 2$). And one HC participant was excluded due to the poor images. In total, 48 participants, including 15 HC, 15 NDPH, and 18 CM participants, were included in this study. Demographics and clinical characteristic data in different groups are summarized in Table 1. All participants were right-handed. No significant differences were found in terms of age, sex, and body mass index. Compared with NDPH patients, CM patients had less frequency of bilateral headache ($P = 0.007$), more severe headache intensity ($P = 0.003$), and a higher frequency of light sensitivity ($P = 0.047$) and vomiting ($P = 0.012$). There were no significant differences in other clinical characteristics among different groups.

Comparison of regional CBF values among HC, NDPH and CM groups

As shown in Table 2, there were significant differences in regional CBF values among HC, NDPH and CM participants (all $P < 0.05$). This study found six brain regions with significant differences in the cerebral cortex and five in the deep nuclei. Compared with HC participants, the CBF was decreased in the right posterior orbital gyrus (OFCpost.R) ($P = 0.023$), right middle occipital gyrus (MOG.R) ($P = 0.002$), and ventral anterior nucleus of the right thalamus (tVA.R) ($P = 0.014$) in the patients with NDPH. In the contrast, for patients with CM, the CBF

Bai *et al. The Journal of Headache and Pain*   (2022) 23:156

Page 5 of 13

Table 1 Demographic characteristics and clinical data of participants in the three groups

	HC (*n* = 15)	CM (*n* = 18)	NDPH (*n* = 15)	*P* value
Age (years)	40.93 ± 9.11	41.61 ± 12.66	44.93 ± 17.15	0.677
Female, *n* (%)	8 (53.3)	11 (61.1)	7 (46.7)	0.707
BMI (kg/m^2)	22.84 ± 2.92	23.44 ± 3.62	23.79 ± 3.63	0.746
Right-handers, *n* (%)	15 (100.0)	18 (100.0)	15 (100.0)	1.000
Headache laterality, *n* (%)				
Unilateral	NA	7 (38.9)	3 (20.0)	0.426
Bilateral	NA	6 (33.3)	12 (80.0)	**0.007****
Shift	NA	5 (27.8)	0 (0.0)	**NA**
Location of headache, *n* (%)				
Frontal region	NA	10 (55.6)	5 (33.3)	0.202
Temporal region	NA	14 (77.8)	11 (73.3)	> 0.999
Parietal region	NA	12 (66.7)	9 (60.0)	0.692
Occipital region	NA	10 (55.6)	6 (40.0)	0.373
Periorbital region	NA	5 (27.8)	0 (0.0)	**NA**
Disease duration (years)	NA	20.44 ± 8.97	14.52 ± 14.23	0.155
Headache frequency, days/month	NA	30.00 (15.75–30.00)	NA	**NA**
Headache intensity[a]	NA	7.44 ± 1.38	5.67 ± 1.84	**0.003****
Light sensitivity, *n* (%)	NA	16 (88.9)	8 (53.3)	**0.047***
Noise sensitivity, *n* (%)	NA	15 (83.3)	9 (60.0)	0.239
Vomiting, *n* (%)	NA	10 (55.6)	2 (13.3)	**0.012***
HIT-6 score (36–78)	NA	64.53 ± 9.64	64.36 ± 9.93	0.962
PHQ-9 score (0–27)	NA	7.50 (3.50–16.00)	10.00 (7.00–17.00)	0.247
GAD-7 score (0–21)	NA	4.50 (2.00–9.75)	6.00 (5.00–10.00)	0.140
PSQI score (0–21)	NA	9.86 ± 4.37	11.50 ± 3.55	0.284

HC healthy control, *NDPH* new daily persistent headache, *CM* chronic migraine, *NA* not applicable. *BMI* body mass index, *HIT-6* Headache Impact Test-6, *PHQ-9* Patient Health Questionnaire-9, *GAD-7* Generalized Anxiety Disorder-7, *PSQI* Pittsburgh Sleep Quality Index, [a] Headache intensity on a 0–10 numerical rating scale. * *P* < 0.05, ** *P* < 0.01

Table 2 Brain regions with significant differences in CBF among different groups

Locations	Brain Regions	CBF (ml/100 g/min)			
		HC (*n* = 15)	CM (*n* = 18)	NDPH (*n* = 15)	*P* value
Cortex	IFGorb.R	58.82 (55.96–71.27)	67.44 (57.93–79.50)	47.88 (43.46–58.29)	0.008**
	OFCpost.R	58.77 (53.01–68.60)	60.67 (57.14–72.10)	46.42 (43.44–56.43)	0.004**
	OFClat.R	49.03 ± 10.00	60.25 ± 17.02	44.26 ± 10.39	0.003**
	ACCsup.R	25.13 (22.59–27.60)	27.22 (24.03–31.80)	21.64 (16.89–27.11)	0.012*
	TPOsup.R	56.32 ± 8.68	56.56 ± 12.11	46.86 ± 11.54	0.026*
	MOG.R	53.10 (46.97–60.14)	54.10 (46.42–68.23)	39.34 (34.91–43.86)	< 0.001***
Nucleus	Amygdala.R	41.31 (39.28–48.45)	46.47 (43.60–57.97)	35.28 (30.33–42.69)	0.002**
	Pallidum.L	41.76 ± 7.52	44.07 ± 8.47	35.54 ± 7.54	0.011*
	tVA.R	35.13 ± 6.04	37.31 ± 7.47	27.76 ± 6.63	0.001**
	tVL.L	38.06 ± 7.89	48.10 ± 7.39	40.08 ± 10.78	0.004**
	tVL.R	33.58 ± 5.04	40.12 ± 6.44	32.17 ± 8.35	0.003**

HC healthy control, *NDPH* new daily persistent headache, *CM* chronic migraine. *IFGorb.R* right inferior frontal gyrus pars orbitalis, *OFCpost.R* right posterior orbital gyrus, *OFClat.R* right lateral orbital gyrus, *ACCsup.R* right anterior cingulate cortex, supracallosal gyrus, *TPOsup.R* right superior temporal gyrus, temporal pole, *MOG.R* right middle occipital gyrus, *Amygdala.R* right amygdala, *Pallidum.L* left pallidum, *tVA.R* right thalamus, ventral anterior nucleus, *tVL.L* left thalamus, ventral lateral nucleus, *tVL.R* right thalamus, ventral lateral nucleus. * *P* < 0.05, ** *P* < 0.01,*** *P* < 0.001

Bai *et al. The Journal of Headache and Pain*   (2022) 23:156

Page 6 of 13

was increased in the ventral lateral nucleus of the left thalamus (tVL.L) ($P = 0.006$) and right thalamus (tVL.R) ($P = 0.023$) compared with HC participants. Compared with CM, the regional CBF was observed to be significantly decreased in NDPH (all $P < 0.05$) (Fig. 2).

Comparison of regional aCBV values among HC, NDPH and CM groups

Significant differences in regional aCBV values among HC, NDPH, and CM participants are presented in Table 3. Compared with HC participants, the aCBV was decreased in the right posterior orbital gyrus (OFCpost.R) ($P = 0.030$), right middle occipital gyrus (MOG.R) ($P = 0.048$), temporal pole of right superior temporal gyrus (TPOsup.R) ($P = 0.034$), and ventral anterior nucleus of the right thalamus (tVA.R) ($P = 0.009$) in patients with NDPH. On the contrary, for patients with CM, the aCBV was raised in the ventral lateral nucleus of the left thalamus (tVL.L) ($P = 0.010$) compared with HC participants. Compared with CM, the regional aCBV was significantly decreased in NDPH (all $P < 0.05$), except in the OFCpost.R, TPOsup.R, and right anterior cingulate cortex, supracallosal gyrus (ACCsup.R) (Fig. 3). As shown in Fig. 4, the visualization of brain regions with significant differences in cerebral perfusion was performed between the NDPH and HC groups, NDPH and CM groups, as well as the CM and HC groups.

Correlation analysis between cerebral perfusion parameters in brain regions with significant differences and clinical variables

For patients with NDPH, the correlation analysis showed that the increased aCBV in the region of IFGorb.R was positively correlated with the GAD-7 score ($r = 0.604$, $P = 0.037$, $n = 15$) after the age and sex adjustments. Meanwhile, the increased CBF ($r = 0.921$, $P < 0.001$, n = 15) and aCBV ($r = 0.765$, $P = 0.004$, $n = 15$) in the tVA.R region were positively correlated with disease duration (Fig. 5). No significant correlation was found between cerebral perfusion parameters and other clinical characteristics in the brain regions with significant differences (all $P > 0.05$). For patients with CM, there were no significant correlations between cerebral perfusion parameters and clinical characteristics in the brain regions with significant differences (all $P > 0.05$).

Discussion

In the present study, we found that, compared with HCs, patients with NDPH showed a decrease in CBF or aCBV values in multiple cortical regions in the right hemisphere, while patients with CM showed an increase in CBF and aCBV values in the bilateral thalamus. These intriguing findings may reveal the different cerebral hemodynamic variations between these two types of primary chronic headache. So far, the underlying neurovascular mechanism of NDPH is still unknown. There has been no report on the cerebral hemodynamic features of patients with NDPH. Only a few structural imaging studies on NDPH was reported. A recent study showed that patients with NDPH had no structural brain changes [36]. Another study of adolescent found that patients with NDPH reduced cortical thickness in the bilateral superior temporal gyrus, left superior, and middle frontal gyrus areas compared with controls [34]. There is still some controversy regarding the alteration of NDPH structure. One previous study of chronic tension-type headache (CTTH) showed a significant gray matter volume decrease in pain processing regions [37]. Meanwhile, Schmidt-Wilcke et al. [37] revealed the brain structural levels are different between patients with CTTH and migraine. Similarly, from the perspective of cerebral perfusion in NDPH and CM, our study found that the different regional perfusion between the two types of primary chronic headache.

Previous studies have reported the cerebral hyperperfusion pattern of episodic migraine (EM) in several brain regions [12, 21, 22]. Another study on tinnitus patients with migraine showed reduced CBF in the temporal and prefrontal cortex [38]. One recent study of CM using 3D pCASL imaging detected hypoperfusion of the left nucleus accumbens [10]. However, cerebral hemodynamic investigation was still rarely reported in CM. The current study showed hyperperfusion in the bilateral thalamus for patients with CM. Thalamus is considered the relay center for ascending nociceptive information [39]. According to functional imaging studies, the increased thalamus neuronal activation during migraine attacks and the overall abnormal functional connectivity in the thalamocortical limb of the trigeminovascular pathway suggested dysfunctional pain processing in migraine [40, 41]. For patients with CM, during the process of migraine chronification, recurring attacks of migraine may lead to increase neuronal activation in the thalamus, which may be one of the reasons for cerebral hyperperfusion in the thalamus. One magnetic resonance spectroscopy (MRS) study in migraineurs revealed significantly increased glutamate/glutamine (GLX) levels in both the primary occipital cortex and right thalamus [42]. The changes in brain tissue metabolism levels might reflect cerebral perfusion variance to some extent.

Altered regional cerebral perfusion may reflect differences in neuronal metabolism or activity. Tumor necrosis factor alpha (TNF-α) is a proinflammatory cytokine involved in central nervous system (CNS) inflammation, immune activity, and pain initiation. Rozen et al. [43] found that 95% of NDPH patients had elevated TNF-α
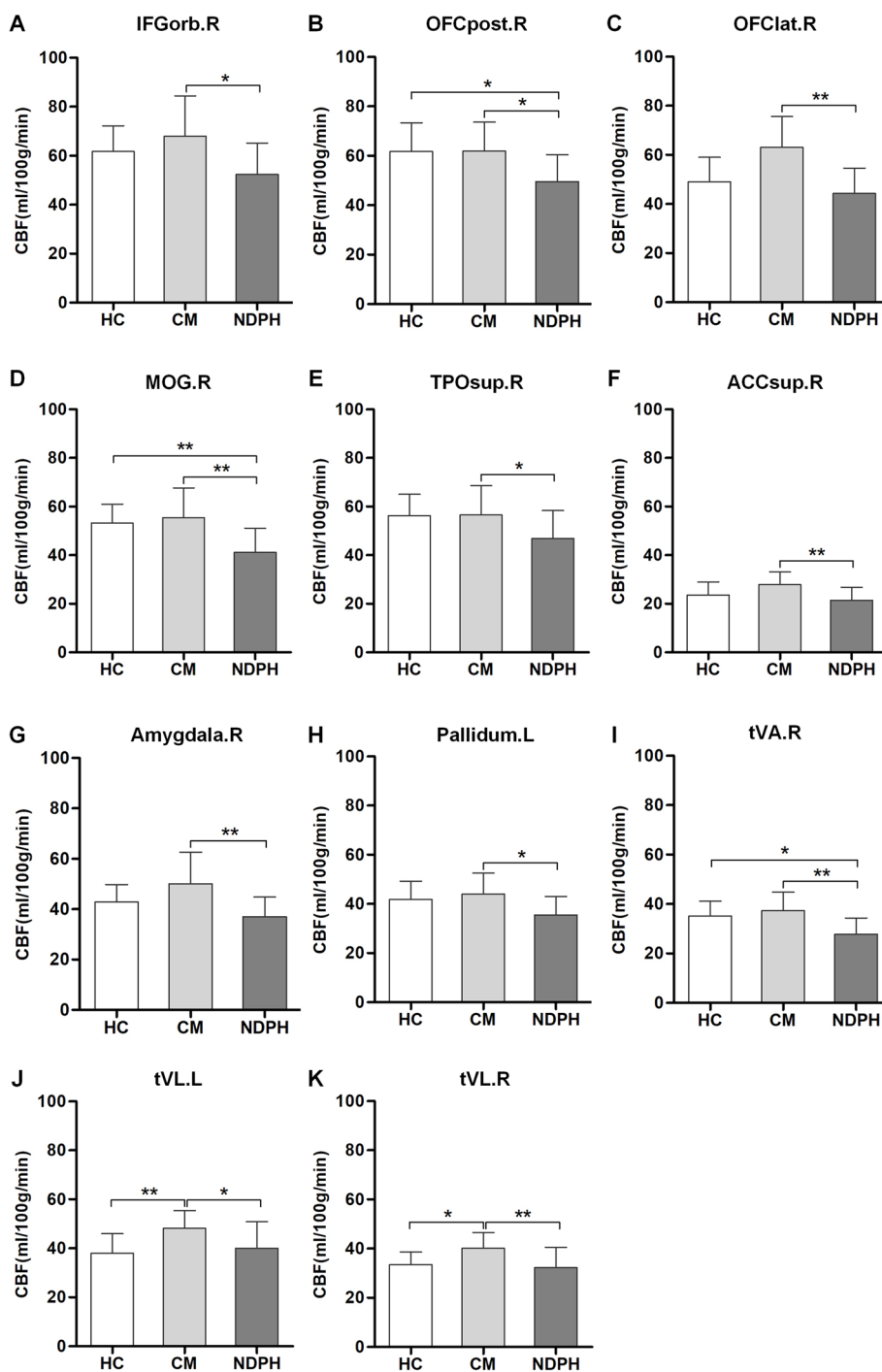
Fig. 2 Brain regions with significant differences in CBF between NDPH and HC groups, NDPH and CM groups, as well as CM and HC groups (**A-K**). *HC* healthy control, *NDPH* new daily persistent headache, *CM* chronic migraine. *IFGorb.R* right inferior frontal gyrus pars orbitalis, *OFCpost.R* right posterior orbital gyrus, *OFClat.R* right lateral orbital gyrus, *ACCsup.R* right anterior cingulate cortex, supracallosal gyrus. *TPOsup.R* right superior temporal gyrus, temporal pole, *MOG.R* right middle occipital gyrus, *Amygdala.R* right amygdala, *Pallidum.L* left pallidum, *tVA.R* right thalamus, ventral anterior nucleus, *tVL.L* left thalamus, ventral lateral nucleus, *tVL.R* right thalamus, ventral lateral nucleus. * *P*<0.05, ** *P*<0.01

Bai *et al. The Journal of Headache and Pain*   (2022) 23:156

Page 8 of 13

Table 3 Brain regions with significant differences in aCBV among different groups

Locations	Regions	aCBV (ml/100 g)			
		HC (*n* = 15)	CM (*n* = 18)	NDPH (*n* = 15)	*P* value
Cortex	IFGorb.R	1.52 ± 0.27	1.58 ± 0.34	1.28 ± 0.29	0.022*
	OFCpost.R	1.39 ± 0.34	1.33 ± 0.22	1.13 ± 0.24	0.024*
	OFClat.R	1.28 ± 0.31	1.50 ± 0.43	1.11 ± 0.25	0.009**
	ACCsup.R	0.48 ± 0.11	0.56 ± 0.13	0.45 ± 0.13	0.043*
	TPOsup.R	1.38 ± 0.24	1.28 ± 0.26	1.12 ± 0.28	0.035*
	MOG.R	1.25 ± 0.18	1.29 ± 0.27	1.04 ± 0.22	0.006**
Nucleus	Amygdala.R	0.88 (0.85–1.12)	1.01 (0.86–1.21)	0.76 (0.69–0.87)	0.002**
	Pallidum.L	0.81 ± 0.17	0.85 ± 0.17	0.69 ± 0.17	0.028*
	tVA.R	0.68 ± 0.14	0.70 ± 0.17	0.52 ± 0.12	0.001**
	tVL.L	0.70 ± 0.13	0.87 ± 0.16	0.73 ± 0.17	0.007**
	tVL.R	0.61 ± 0.10	0.71 ± 0.13	0.59 ± 0.14	0.009**

HC healthy control, *NDPH* new daily persistent headache, *CM* chronic migraine. *IFGorb.R* right inferior frontal gyrus pars orbitalis, *OFCpost.R* right posterior orbital gyrus, *OFClat.R* right lateral orbital gyrus, *ACCsup.R* right anterior cingulate cortex, supracallosal gyrus, *TPOsup.R* right superior temporal gyrus, temporal pole, *MOG.R* right middle occipital gyrus, *Amygdala.R* right amygdala, *Pallidum.L* left pallidum, *tVA.R* right thalamus, ventral anterior nucleus, *tVL.L* left thalamus, ventral lateral nucleus, *tVL.R* right thalamus, ventral lateral nucleus. * $P < 0.05$, ** $P < 0.01$

levels in cerebrospinal fluid (CSF) and suggested a role of TNF-α in the pathogenesis of NDPH. Calcitonin gene-related peptide (CGRP) is a known factor in the migraine pathogenesis cascade [44]. Previous evidence showed that TNF-α would induce CGRP production [45]. It has been speculated that intracranial TNF-α receptors are located in trigeminal ganglion neurons, and the release of TNF-α leads to an increase in CGRP levels. CGRP has been confirmed to cause the vasodilation of meninges and intracranial arteries and contribute to neurogenic inflammation by triggering the release of neuron sensitizing agents from mast cells [44, 46, 47]. As a pain factor, it participates in the transmission of intracranial blood vessels to trigeminal sensory nerve signals, leading to headache attacks. Regarding NDPH, reduced cortical cerebral perfusion may be associated with compensatory vasoconstriction due to persistent headache. A previous study reported two cases of NDPH-like headaches after acute bouts of reversible cerebral vasoconstriction syndrome (RCVS), which suggested that vasoconstriction in RCVS may be regarded as a trigger for NDPH-like headache [48]. In addition, the persistence of headache attacks might accelerate the decreased cerebral perfusion in NDPH. This is an initial observation that must be substantiated by future studies.

In our study, we found that the hypoperfusion brain regions in NDPH were lateralized to the right hemisphere, which was similar to the previous studies showing that abnormal cerebral perfusion regions in episodic migraine were lateralized to the right cortex [12, 22]. A previous multimodal MRI study of neurovascular coupling (NVC) dysfunction in CM showed that NVC

biomarkers were significantly higher in right superior occipital gyrus, right superior parietal gyrus, and precuneus, which was considered the compensatory response [49]. One survey of 188 consecutive chronic headache patients reported that about 50% of headache cases were lateralized with an overall right-sided predominance (59%) [50]. One recent study reported that 62.8% of unilateral pain episodes occurred on the right side for right-handed migraine patients. This study suggested that the manual dominance of participants with migraine may strongly influence pain lateralization [51]. All patients with NDPH in this study were right-handed, which may be one of the causes of hypoperfusion in the right hemisphere. However, more frequency of bilateral headaches was presented in patients with NDPH in this study. Therefore, the lateralization of hypoperfusion brain regions in patients with NDPH needs to be investigated and verified in future studies.

In the present study, NDPH patients exhibited a decreased cerebral perfusion in the prefrontal cortex (PFC), including IFGorb.R and OFCpost.R, which are the critical areas of reward, decision making, and emotion regulation [52, 53]. A previous study revealed that NDPH is linked to anxiety and panic disorders [54]. Patients with NDPH showed defects in emotional expression after impaired PFC function. Our study found that the increased aCBV of IFGorb.R was positively correlated with the GAD-7 score in NDPH, which were similar to a previous study [55]. In addition, the increased CBF and aCBV of tVA.R were positively correlated with disease duration. A possible explanation is that with the prolongation of the disease duration, NDPH manifested as
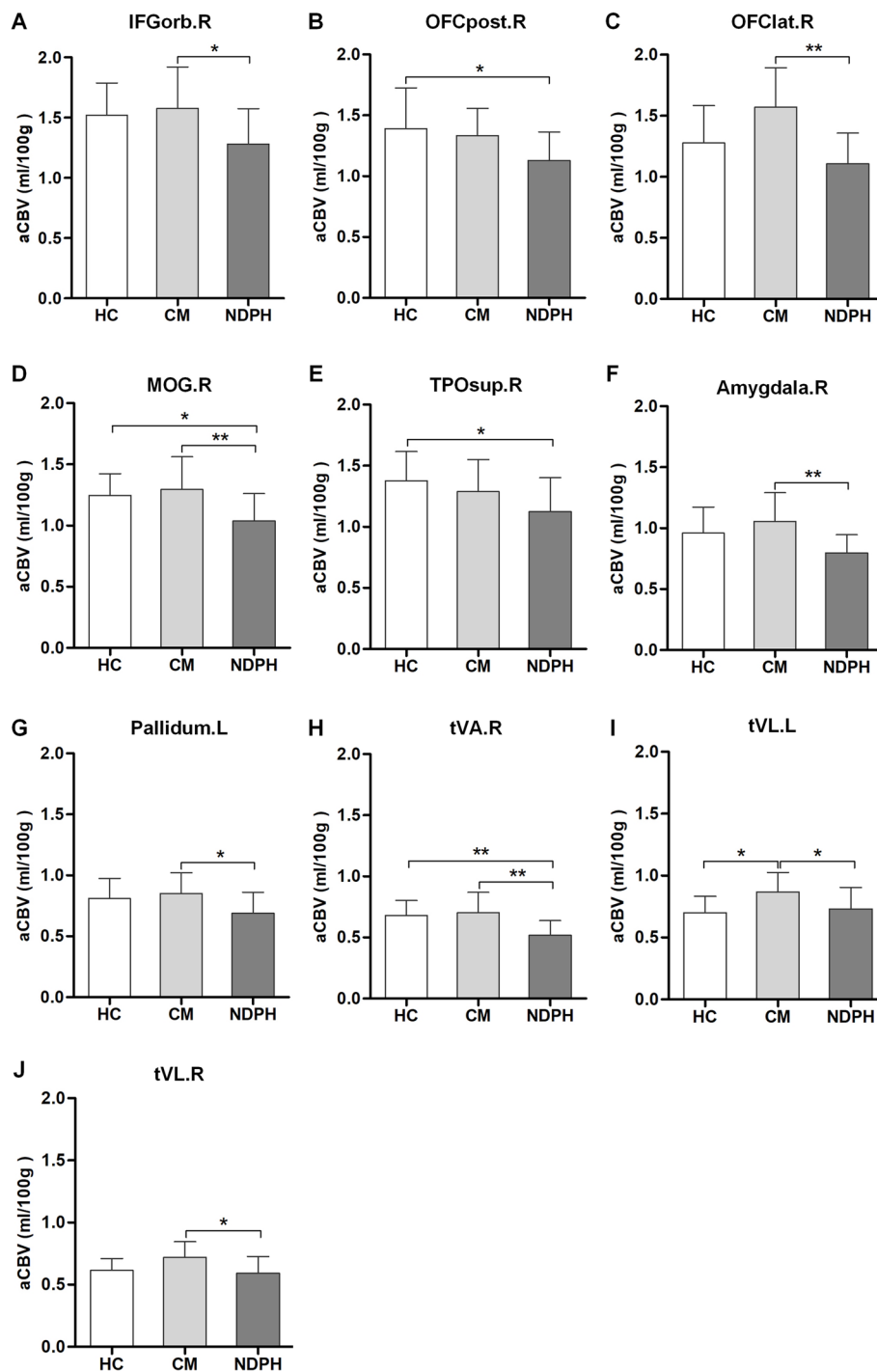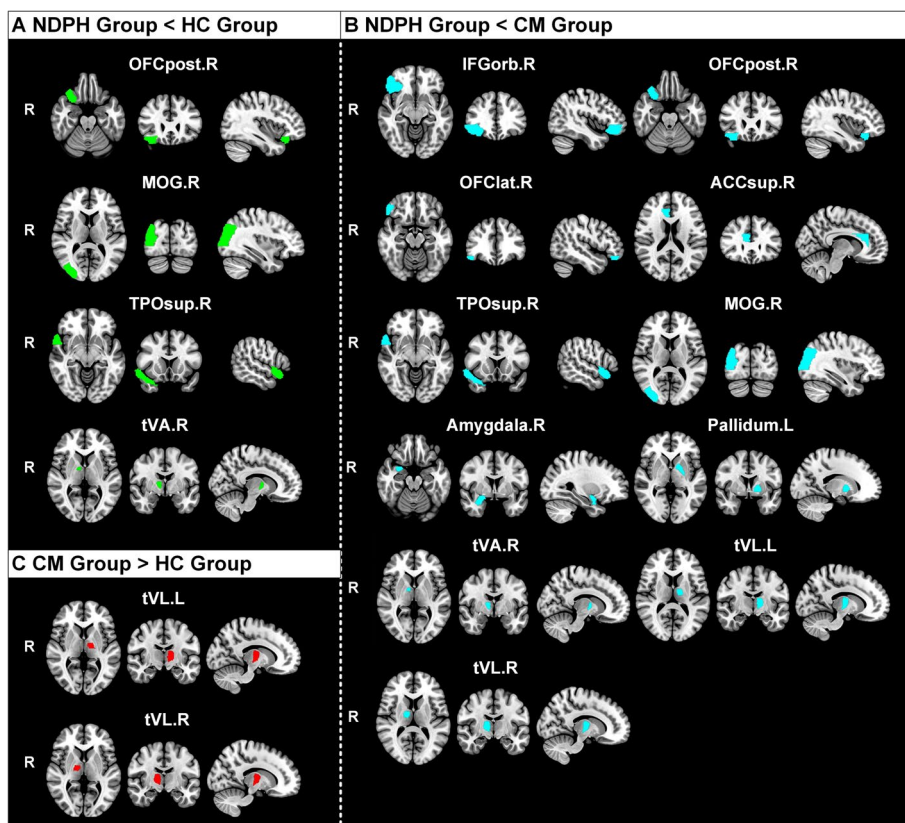
Fig. 3 Brain regions with significant differences in the aCBV between NDPH and HC groups, NDPH and CM groups, as well as CM and HC groups (**A-J**). *HC* healthy control, *NDPH* new daily persistent headache, *CM* chronic migraine. *IFGorb.R* right inferior frontal gyrus pars orbitalis, *OFCpost.R* right posterior orbital gyrus, *OFClat.R* right lateral orbital gyrus, *TPOsup.R* right superior temporal gyrus, temporal pole, *MOG.R* right middle occipital gyrus, *Amygdala.R* right amygdala, *Pallidum.L* left pallidum, *tVA.R* right thalamus, ventral anterior nucleus, *tVL.L* left thalamus, ventral lateral nucleus, *tVL.R* right thalamus, ventral lateral nucleus. * $P<0.05$, ** $P<0.01$

Bai *et al. The Journal of Headache and Pain*   (2022) 23:156

Page 10 of 13

Fig. 4 The visualization of brain regions with significant differences in cerebral perfusion between NDPH and HC groups, CM and HC groups, as well as NDPH and CM groups. The brain regions with decreased cerebral perfusion in NDPH groups were presented compared with HC (**A**) and CM (**B**) groups, respectively. The brain regions with increased cerebral perfusion in CM groups were presented compared with HC groups (**C**). *HC* healthy control, *NDPH* new daily persistent headache, *CM* chronic migraine. *IFGorb.R* right inferior frontal gyrus pars orbitalis, *OFCpost.R* right posterior orbital gyrus, *OFClat.R* right lateral orbital gyrus, *ACCsup.R* right anterior cingulate cortex, supracallosal gyrus, *TPOsup.R* right superior temporal gyrus, temporal pole, *MOG.R* right middle occipital gyrus, *Amygdala.R* right amygdala, *Pallidum.L* left pallidum, *tVA.R* right thalamus, ventral anterior nucleus, *tVL.L* left thalamus, ventral lateral nucleus, *tVL.R* right thalamus, ventral lateral nucleus
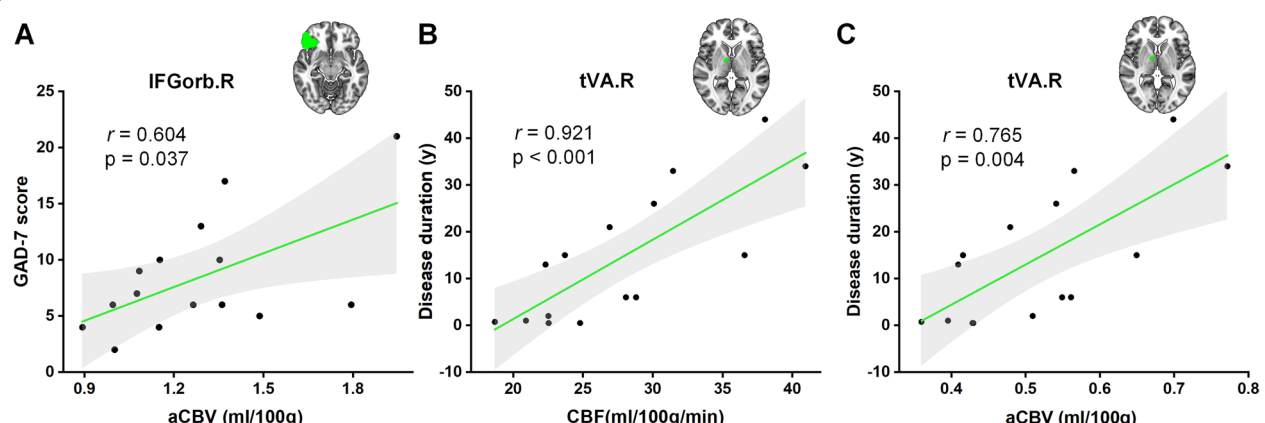
Fig. 5 Correlation analysis between cerebral perfusion parameters and clinical variables in brain regions with significant differences of NDPH. The aCBV of the right inferior frontal gyrus pars orbitalis (IFGorb.R) was positively correlated with the GAD-7 score (**A**). The CBF of the right thalamus, ventral anterior nucleus (tVA.R) was positively correlated with disease duration (**B**), as well as the aCBV of tVA.R (**C**). *NDPH* new daily persistent headache, *aCBV* arterial cerebral blood volume, *CBF* cerebral blood flow, *GAD-7* Generalized Anxiety Disorder-7

Bai *et al. The Journal of Headache and Pain*   (2022) 23:156

Page 11 of 13

a decreased vasoconstriction response, and the chronification process of NDPH may be a possible reason for the increased regional cerebral perfusion. However, the pathogenesis of NDPH and the relationship between cerebral perfusion and clinical features have not been clearly reported. Our findings need to be confirmed by future studies.

The present study used multi-delay pCASL MR imaging, a novel non-enhancement perfusion sequence, to detect changes in cerebral perfusion of NDPH and CM. As far as we know, it is the first study to utilize multi-delay pCASL MRI for assessing the cerebral perfusion of NDPH. Multi-delay pCASL, in which images with several post-label delay times are acquired, has several potential advantages over existing single delay ASL scans, including improved accuracy of CBF quantification, imaging of multiple hemodynamic parameters (ATT, and CBF), and better visualization of collateral flow through dynamic image series [31]. Previous ASL studies generally employed a single post-labeling delay (PLD) time typically between 1.5 and 2 s for the estimation of CBF [10, 12]. However, prolonged ATT may result in underestimation of CBF in brain tissue. In this study, we encoded seven different PLD times with the application of seven effective label durations. Many studies on cerebrovascular disease have utilized multi-delay ASL approaches to correct CBF values for arrival time [56–58]. It was demonstrated that the multi-delay ASL technique holds an advantage for clinical applications, particularly for patients with arterial transit time abnormalities.

There were several limitations to our study. First, the sample size was relatively small, which might lead to the resulting bias in this study. However, NDPH cases are not common in clinical practice. Also, patients with NDPH had a wide range of headache duration, which caused the heterogeneity of patients. But there was no significant difference in the headache duration between the NDPH and CM groups in this study. Nonetheless, the small sample size and heterogeneity of patients may affect the generalizability of these results. This was a preliminary study to investigate the cerebral perfusion variance of NDPH and CM. We will increase the sample size to verify the accuracy and generalization of the results in future studies. In addition, it was a cross-sectional study, with only CM without aura included. Further studies will follow with a focus on the dynamic perfusion changes during different phases of a CM attack and post-attack. Moreover, the spatial resolution of ASL imaging used in the current study was 1.6 mm × 1.6 mm × 4.0 mm, which made it impossible to investigate the changes in the substructure of small nuclei. However, improving the spatial resolution will significantly decrease the SNR and prolong the acquisition time. Further technical development of ASL techniques is necessary to improve the accuracy of perfusion parameter quantification.

Conclusion

The multi-delay pCASL technique can detect cerebral perfusion variation in patients with NDPH and CM. The cerebral perfusion changes may suggest different variations between NDPH and CM, which might provide hemodynamic evidence of these two types of primary headaches.

Abbreviations

HC: Healthy control; NDPH: New daily persistent headache; CM: Chronic migraine; EM: Episodic migraine; CTTH: Chronic tension-type headache; pCASL: Pseudo-continuous arterial labeling; PLD: Post-label delay; CBF: Cerebral blood flow; ATT: Arterial transit time; aCBV: Arterial cerebral blood volume; IFGorb.R: Right inferior frontal gyrus pars orbitalis; OFCpost.R: Right posterior orbital gyrus; OFClat.R: Right lateral orbital gyrus; ACCsup.R: Right anterior cingulate cortex, supracallosal gyrus; TPOsup.R: Right superior temporal gyrus, temporal pole; MOG.R: Right middle occipital gyrus; Amygdala.R: Right amygdala; Pallidum.L: Left pallidum; tVA.R: Right thalamus, ventral anterior nucleus; tVL.L: Left thalamus, ventral lateral nucleus; tVL.R: Right thalamus, ventral lateral nucleus; HIT-6: Headache Impact Test-6; PHQ-9: Patient Health Questionnaire-9; GAD-7: Generalized Anxiety Disorder-7; PSQI: Pittsburgh Sleep Quality Index; TNF-α: Tumor necrosis factor alpha; CGRP: Calcitonin gene-related peptide; RCVS: Cerebral vasoconstriction syndrome; CSF: Cerebrospinal fluid; SNR: Signal-to-noise ratio; PET: Positron emission tomography; DSC: Dynamic susceptibility contrast; ICHD-3: International Classification of Headache Diseases, 3rd edition; MNI: Montreal Neurologic Institute; SPM 12: Statistical Parametric Mapping 12; AAL3: Automated anatomical labelling atlas 3; MRI: Magnetic resonance imaging; ANOVA: One-way analysis of variance; MRS: Magnetic resonance spectroscopy; GLX: Glutamate/glutamine; CNS: Central nervous system; NVC: Neurovascular coupling; PFC: Prefrontal cortex.

Supplementary Information

The online version contains supplementary material available at https://doi.org/10.1186/s10194-022-01532-7.

> **Additional file 1: Supplementary Fig. 1.** The patient enrollment flowchart.

Authors' contributions

XYB, WW, BBS, and YGW supported the conception and design of this project. XYZ, XZ, ZYL, ZYY, PZ, HFT, YQZ, and XYY acquired data. XYB and ZXH analyzed the data. YKZ and ZXH contributed to data quality control. XYB produced the first draft. All authors contributed intellectual content to the revised manuscript and have read and approved the final manuscript.

Availability of data and materials

Data can be made available upon request.

Bai *et al. The Journal of Headache and Pain*   (2022) 23:156

Page 12 of 13

Declarations

Ethics approval and consent to participate

Consent for publication
All authors have agreed to the current submission.

Competing interests
The authors declare that they have no competing interests.

Author details
[1]Tiantan Neuroimaging Center for Excellence, China National Clinical Research Center for Neurological Diseases, Beijing Tiantan Hospital, Capital Medical University, No.119 South Fourth Ring West Road, Fengtai District, Beijing 100070, China. [2]Department of Radiology, Beijing Tiantan Hospital, Capital Medical University, No.119 South Fourth Ring West Road, Fengtai District, Beijing 100070, China. [3]Headache Center, Department of Neurology, Beijing Tiantan Hospital, Capital Medical University, No.119 South Fourth Ring West Road, Fengtai District, Beijing 100070, China. [4]Department of Neurology, The First Affiliated Hospital of Zhengzhou University, No.1 Jianshe East Road, Zhengzhou, Henan Province 450000, China. [5]GE Healthcare, No.1 Tongji Nan Road, Beijing Economic Technological Development Area, Beijing 100176, China.

References

1. (IHS) HCCotIHS (2018) Headache classification Committee of the International Headache Society (IHS) the international classification of headache disorders. Cephalalgia 38:1–211
2. Yamani N, Olesen J (2019) New daily persistent headache: a systematic review on an enigmatic disorder. J Headache Pain 20:80
3. Grande RB, Aaseth K, Lundqvist C, Russell MB (2009) Prevalence of new daily persistent headache in the general population. The Akershus study of chronic headache. Cephalalgia 29:1149–1155
4. Uniyal R, Paliwal VK, Tripathi A (2017) Psychiatric comorbidity in new daily persistent headache: a cross-sectional study. Eur J Pain 21:1031–1038
5. Stovner LJ, Hagen K, Linde M, Steiner TJ (2022) The global prevalence of headache: an update, with analysis of the influences of methodological factors on prevalence estimates. J Headache Pain 23:34
6. May A, Schulte LH (2016) Chronic migraine: risk factors, mechanisms and treatment. Nat Rev Neurol 12:455–464
7. Su M, Yu S (2018) Chronic migraine: a process of dysmodulation and sensitization. Mol Pain 14:1744806918767697
8. Mason BN, Russo AF (2018) Vascular contributions to migraine: time to revisit? Front Cell Neurosci 12:233
9. Hoffmann J, Baca SM, Akerman S (2019) Neurovascular mechanisms of migraine and cluster headache. J Cereb Blood Flow Metab 39:573–594
10. Liu M, Sun Y, Li X, Chen Z (2022) Hypoperfusion in nucleus accumbens in chronic migraine using 3D pseudo-continuous arterial spin labeling imaging MRI. J Headache Pain 23:72
11. Fu T, Liu L, Huang X, Zhang D, Gao Y, Yin X, Lin H, Dai Y, Wu X (2022) Cerebral blood flow alterations in migraine patients with and without aura: An arterial spin labeling study. J Headache Pain 23:131
12. Zhang D, Huang X, Mao C, Chen Y, Miao Z, Liu C, Xu C, Wu X, Yin X (2021) Assessment of normalized cerebral blood flow and its connectivity with migraines without aura during interictal periods by arterial spin labeling. J Headache Pain 22:72
13. Xu G, Rowley HA, Wu G, Alsop DC, Shankaranarayanan A, Dowling M, Christian BT, Oakes TR, Johnson SC (2010) Reliability and precision of pseudo-continuous arterial spin labeling perfusion MRI on 3.0 T and comparison with 15O-water PET in elderly subjects at risk for Alzheimer's disease. NMR Biomed 23:286–293
14. Wolf ME, Okazaki S, Eisele P, Rossmanith C, Gregori J, Griebe M, Gunther M, Gass A, Hennerici MG, Szabo K, Kern R (2018) Arterial spin labeling cerebral perfusion magnetic resonance imaging in migraine Aura: An observational study. J Stroke Cerebrovasc Dis 27:1262–1266
15. Rischka L, Godbersen GM, Pichler V, Michenthaler P, Klug S, Klobl M, Ritter V, Wadsak W, Hacker M, Kasper S, Lanzenberger R, Hahn A (2021) Reliability of task-specific neuronal activation assessed with functional PET, ASL and BOLD imaging. J Cereb Blood Flow Metab 41:2986–2999
16. Haller S, Zaharchuk G, Thomas DL, Lovblad KO, Barkhof F, Golay X (2016) Arterial spin labeling perfusion of the brain: emerging clinical applications. Radiology 281:337–356
17. Alsop DC, Detre JA, Golay X, Gunther M, Hendrikse J, Hernandez-Garcia L, Lu H, MacIntosh BJ, Parkes LM, Smits M, van Osch MJ, Wang DJ, Wong EC, Zaharchuk G (2015) Recommended implementation of arterial spin-labeled perfusion MRI for clinical applications: a consensus of the ISMRM perfusion study group and the European consortium for ASL in dementia. Magn Reson Med 73:102–116
18. Di Napoli A, Cheng SF, Gregson J, Atkinson D, Markus JE, Richards T, Brown MM, Sokolska M, Jager HR (2020) Arterial spin labeling MRI in carotid stenosis: arterial transit artifacts May predict symptoms. Radiology 297:652–660
19. Bambach S, Smith M, Morris PP, Campeau NG, Ho ML (2022) Arterial spin labeling applications in pediatric and adult neurologic disorders. J Magn Reson Imaging 55:698–719
20. Yoo RE, Yun TJ, Hwang I, Hong EK, Kang KM, Choi SH, Park CK, Won JK, Kim JH, Sohn CH (2020) Arterial spin labeling perfusion-weighted imaging aids in prediction of molecular biomarkers and survival in glioblastomas. Eur Radiol 30:1202–1211
21. Chen Z, Chen X, Liu M, Liu M, Ma L, Yu S (2018) Evaluation of gray matter perfusion in episodic migraine using voxel-wise comparison of 3D pseudo-continuous arterial spin labeling. J Headache Pain 19:36
22. Michels L, Villanueva J, O'Gorman R, Muthuraman M, Koirala N, Buchler R, Gantenbein AR, Sandor PS, Luechinger R, Kollias S, Riederer F (2019) Interictal Hyperperfusion in the higher visual cortex in patients with episodic migraine. Headache 59:1808–1820
23. Xu X, Tan Z, Fan M, Ma M, Fang W, Liang J, Xiao Z, Shi C, Luo L (2021) Comparative study of multi-delay Pseudo-continuous arterial spin labeling perfusion MRI and CT perfusion in ischemic stroke disease. Front Neuroinform 15:719719
24. Wang R, Yu S, Alger JR, Zuo Z, Chen J, Wang R, An J, Wang B, Zhao J, Xue R, Wang DJ (2014) Multi-delay arterial spin labeling perfusion MRI in moyamoya disease--comparison with CT perfusion imaging. Eur Radiol 24:1135–1144
25. Chen G, Lei D, Ren J, Zuo P, Suo X, Wang DJ, Wang M, Zhou D, Gong Q (2016) Patterns of postictal cerebral perfusion in idiopathic generalized epilepsy: a multi-delay multi-parametric arterial spin labelling perfusion MRI study. Sci Rep 6:28867
26. Shin HE, Park JW, Kim YI, Lee KS (2008) Headache impact Test-6 (HIT-6) scores for migraine patients: their relation to disability as measured from a headache diary. J Clin Neurol 4:158–163
27. Levis B, Benedetti A, Thombs BD (2019) Accuracy of patient health Questionnaire-9 (PHQ-9) for screening to detect major depression: individual participant data meta-analysis. BMJ 365:l1476
28. Plummer F, Manea L, Trepel D, McMillan D (2016) Screening for anxiety disorders with the GAD-7 and GAD-2: a systematic review and diagnostic metaanalysis. Gen Hosp Psychiatry 39:24–31
29. Buysse DJ, Reynolds CF, Monk TH, Berman SR, Kupfer DJ (1989) The Pittsburgh sleep quality index: a new instrument for psychiatric practice and research. Psychiatry Res 28:193–213
30. Dai W, Robson PM, Shankaranarayanan A, Alsop DC (2012) Reduced resolution transit delay prescan for quantitative continuous arterial spin labeling perfusion imaging. Magn Reson Med 67:1252–1265
31. Wang DJ, Alger JR, Qiao JX, Gunther M, Pope WB, Saver JL, Salamon N, Liebeskind DS, Investigators US (2013) Multi-delay multi-parametric arterial spin-labeled perfusion MRI in acute ischemic stroke - comparison with dynamic susceptibility contrast enhanced perfusion imaging. Neuroimage Clin 3:1–7
32. Rolls ET, Huang CC, Lin CP, Feng J, Joliot M (2020) Automated anatomical labelling atlas 3. Neuroimage 206:116189
33. Cadiot D, Longuet R, Bruneau B, Treguier C, Carsin-Vu A, Corouge I, Gomes C, Proisy M (2018) Magnetic resonance imaging in children

Bai *et al. The Journal of Headache and Pain*   (2022) 23:156

Page 13 of 13

presenting migraine with aura: association of hypoperfusion detected by arterial spin labelling and vasospasm on MR angiography findings. Cephalalgia 38:949–958

34. Szabo E, Chang YC, Shulman J, Sieberg CB, Sethna NF, Borsook D, Holmes SA, Lebel AA (2022) Alterations in the structure and function of the brain in adolescents with new daily persistent headache: a pilot MRI study. Headache 62:858–869

35. Armstrong RA (2014) When to use the Bonferroni correction. Ophthalmic Physiol Opt 34:502–508

36. Naegel S, Zeller J, Hougard A, Weise CM, Hans Christoph D, Zuelow S, Kleinschnitz C, Obermann M, Solbach K, Holle D (2022) No structural brain alterations in new daily persistent headache - a cross sectional VBM/SBM study. Cephalalgia 42:335–344

37. Schmidt-Wilcke T, Leinisch E, Straube A, Kampfe N, Draganski B, Diener HC, Bogdahn U, May A (2005) Gray matter decrease in patients with chronic tension type headache. Neurology 65:1483–1486

38. Xu ZG, Xu JJ, Chen YC, Hu J, Wu Y, Xue Y (2021) Aberrant cerebral blood flow in tinnitus patients with migraine: a perfusion functional MRI study. J Headache Pain 22:61

39. Younis S, Hougaard A, Noseda R, Ashina M (2019) Current understanding of thalamic structure and function in migraine. Cephalalgia 39:1675–1682

40. Xue T, Yuan K, Cheng P, Zhao L, Zhao L, Yu D, Dong T, von Deneen KM, Gong Q, Qin W, Tian J (2013) Alterations of regional spontaneous neuronal activity and corresponding brain circuit changes during resting state in migraine without aura. NMR Biomed 26:1051–1058

41. Coppola G, Di Renzo A, Tinelli E, Lepre C, Di Lorenzo C, Di Lorenzo G, Scapeccia M, Parisi V, Serrao M, Colonnese C, Schoenen J, Pierelli F (2016) Thalamo-cortical network activity between migraine attacks: insights from MRI-based microstructural and functional resting-state network correlation analysis. J Headache Pain 17:100

42. Bathel A, Schweizer L, Stude P, Glaubitz B, Wulms N, Delice S, Schmidt-Wilcke T (2018) Increased thalamic glutamate/glutamine levels in migraineurs. J Headache Pain 19:55

43. Rozen T, Swidan SZ (2007) Elevation of CSF tumor necrosis factor alpha levels in new daily persistent headache and treatment refractory chronic migraine. Headache 47:1050–1055

44. Iyengar S, Johnson KW, Ossipov MH, Aurora SK (2019) CGRP and the trigeminal system in migraine. Headache 59:659–681

45. Durham PL (2006) Calcitonin gene-related peptide (CGRP) and migraine. Headache 46(1):S3–S8

46. Wattiez AS, Sowers LP, Russo AF (2020) Calcitonin gene-related peptide (CGRP): role in migraine pathophysiology and therapeutic targeting. Expert Opin Ther Targets 24:91–100

47. Iyengar S, Ossipov MH, Johnson KW (2017) The role of calcitonin gene-related peptide in peripheral and central pain mechanisms including migraine. Pain 158:543–559

48. Ling YH, Wang YF, Lirng JF, Fuh JL, Wang SJ, Chen SP (2021) Post-reversible cerebral vasoconstriction syndrome headache. J Headache Pain 22:14

49. Hu B, Yu Y, Dai YJ, Feng JH, Yan LF, Sun Q, Zhang J, Yang Y, Hu YC, Nan HY, Zhang XN, Zheng Z, Qin P, Wei XC, Cui GB, Wang W (2019) Multi-modal MRI reveals the neurovascular coupling dysfunction in chronic migraine. Neuroscience 419:72–82

50. De Benedittis G (1987) Headache lateralization and functional cerebral asymmetry: a task-related EEG power spectrum analysis. J Neurosurg Sci 31:109–119

51. La Pegna GB, Quatrosi G, Vetri L, Reina F, Galati C, Manzo ML, Nocera GM, Brighina F, Raieli V (2021) Migraine and handedness. Neurol Sci 42:2965–2968

52. Dixon ML, Thiruchselvam R, Todd R, Christoff K (2017) Emotion and the prefrontal cortex: An integrative review. Psychol Bull 143:1033–1081

53. Rudebeck PH, Rich EL (2018) Orbitofrontal cortex. Curr Biol 28:R1083–R1088

54. Peres MF, Lucchetti G, Mercante JP, Young WB (2011) New daily persistent headache and panic disorder. Cephalalgia 31:250–253

55. Van den Bergh O, Zaman J, Bresseleers J, Verhamme P, Van Diest I (2013) Anxiety, pCO2 and cerebral blood flow. Int J Psychophysiol 89:72–77

56. Luciw NJ, Shirzadi Z, Black SE, Goubran M, MacIntosh BJ (2022) Automated generation of cerebral blood flow and arterial transit time maps from multiple delay arterial spin-labeled MRI. Magn Reson Med 88:406–417

57. Martin SZ, Madai VI, von Samson-Himmelstjerna FC, Mutke MA, Bauer M, Herzig CX, Hetzer S, Gunther M, Sobesky J (2015) 3D GRASE pulsed arterial spin labeling at multiple inflow times in patients with long arterial transit times: comparison with dynamic susceptibility-weighted contrast-enhanced MRI at 3 tesla. J Cereb Blood Flow Metab 35:392–401

58. Zhao MY, Fan AP, Chen DY, Ishii Y, Khalighi MM, Moseley M, Steinberg GK, Zaharchuk G (2022) Using arterial spin labeling to measure cerebrovascular reactivity in Moyamoya disease: insights from simultaneous PET/MRI. J Cereb Blood Flow Metab 42:1493–1506

Publisher's Note